Table S1. Random inconsistency indices (RI) for N (number of criteria), source: Satty 1980

| N | 1 | 2 | 3 | 4 | 5 | 6 | 7 | 8 | 9 | 10 |
|---|---|---|---|---|---|---|---|---|---|---|
| RI | 0.00 | 0.00 | 0.58 | 0.9 | 1.12 | 1.24 | 1.32 | 1.41 | 1.46 | 1.49 |

## (1) Error matrices for the three classified LULC maps

Table S2. Error matrix for the classified LULC map of 1991

| 1991 | Class types determined from Reference Source | | | | | User's% |
|---|---|---|---|---|---|---|
| Class types determined from Classified Map | | Vegetation | Built-up | Water | ∑ | |
| | Vegetation | 842 | 21 | 5 | 868 | 97.0 |
| | Built-up | 20 | 84 | 0 | 104 | 80.7 |
| | Water | 5 | 0 | 23 | 28 | 82.1 |
| | ∑ | 867 | 105 | 28 | 1000 | |
| | Producer's % | 97.1 | 80.0 | 82.1 | | |

O.A= 94.9% kappa= 0.78

Table S3. Error matrix for the classified LULC map of 2003

| 2003 | Class types determined from Reference Source | | | | | User's% |
|---|---|---|---|---|---|---|
| Class types determined from Classified Map | | Vegetation | Built-up | Water | ∑ | |
| | Vegetation | 814 | 27 | 3 | 844 | 96.4 |
| | Built-up | 19 | 114 | 0 | 133 | 85.7 |
| | Water | 4 | 0 | 19 | 23 | 82.6 |
| | ∑ | 837 | 141 | 22 | 1000 | |
| | Producer's% | 97.2 | 80.9 | 86.4 | | |

O.A= 94.7% kappa= 0.81

Table S4. Error matrix for the classified LULC map of 2018

| 2018 | | Class types determined from Reference Source | | | | User's% |
|---|---|---|---|---|---|---|
| | | Vegetation | Built-up | Water | ∑ | |
| Class types determined from Classified Map | Vegetation | 771 | 36 | 3 | 810 | 95.1 |
| | Built-up | 14 | 157 | 0 | 171 | 91.8 |
| | Water | 1 | 0 | 18 | 19 | 94.7 |
| | ∑ | 786 | 193 | 21 | 1000 | |
| | Producer's% | 98.1 | 81.3 | 85.7 | | |

O.A= 94.6% kappa= 0.84

## Analysis of CA-Markov chain model

Based on the concept of Markov probability, the successive state vectors of 1991 and 2003 (transition through time step of 12 years) reveals a transition probability matrix of changing to each other class and an expected transition area matrix (the area is in pixels) as follows:

Table S5. Transition probability matrix for a time step of 12 years based on LULC of 1991–2003

| | Agricultural land | Built-up | Water |
|---|---|---|---|
| Agricultural land | 0.8216 | 0.1411 | 0.0374 |
| Built-up | 0.2480 | 0.7514 | 0.0005 |
| Water | 0.1695 | 0.0133 | 0.8172 |

Table S6. Transition area matrix for a time step of 12 years based on LULC of 1991–2003

| | Agricultural land | Built-up | Water |
|---|---|---|---|
| Agricultural land | 1626248 | 279227 | 73948 |
| Built-up | 53293 | 161450 | 109 |
| Water | 4610 | 363 | 22227 |

According to the available cloud-free images, CA-Markov model was employed to extract the transition potentials for 2018 (a time step of 15 years) based on the past LULC of 1991 and 2003. The transition probability and transition area matrices for 2018 as follows:

Table S7. Transition probability matrix for 2018 based on past LULC of 1991–2003

| | Agricultural land | Built-up | Water |
|---|---|---|---|
| Agricultural land | 0.8148 | 0.1463 | 0.0389 |
| Built-up | 0.2713 | 0.7281 | 0.0007 |
| Water | 0.1767 | 0.0141 | 0.8092 |

Table S8. Expected transition area (in pixels) matrix for 2018 based on LULC of 1991–2003

| | Agricultural land | Built-up | Water |
|---|---|---|---|
| Agricultural land | 1612857 | 289550 | 77016 |
| Built-up | 58285 | 156425 | 142 |
| Water | 4807 | 383 | 22010 |

The transition probability matrices for LULCC in 2033 and 2048 are elucidated as follows:

Table S9. Transition probability matrix for 2033 based on past LULC of 2003-2018

| | Agricultural land | Built-up | Water |
|---|---|---|---|
| Agricultural land | 0.7924 | 0.2035 | 0.0041 |
| Built-up | 0.1845 | 0.8144 | 0.0002 |
| Water | 0.3265 | 0.0075 | 0.6660 |

Table S10. Expected transition area matrix for 2033 based on LULC of 2003-2018

| | Agricultural land | Built-up | Water |
|---|---|---|---|
| Agricultural land | 1473874 | 378572 | 7579 |
| Built-up | 62570 | 274848 | 77 |
| Water | 7821 | 181 | 15953 |

Table S11. Transition probability matrix for 2048 based on past LULC of 2003-2018

| | Agricultural land | Built-up | Water |
|---|---|---|---|
| Agricultural land | 0.7413 | 0.2541 | 0.0046 |
| Built-up | 0.2170 | 0.7826 | 0.0004 |
| Water | 0.4500 | 0.0280 | 0.5220 |

Table S12. Expected transition area matrix for 2048 based on LULC of 2003-2018

| | Agricultural land | Built-up | Water |
|---|---|---|---|
| Agricultural land | 1378831 | 472594 | 8600 |
| Built-up | 73233 | 264127 | 134 |
| Water | 10780 | 670 | 12505 |

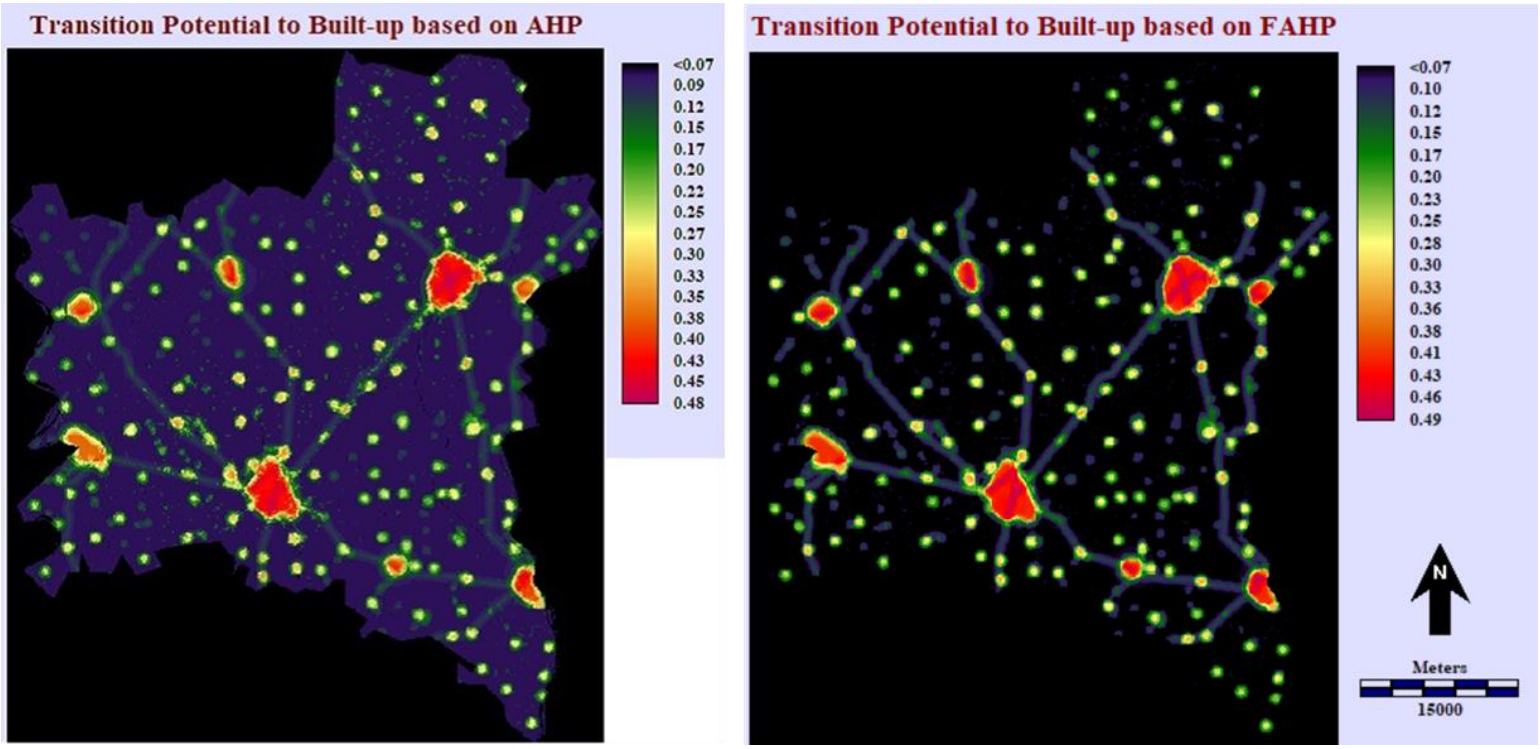


Figure S1. Transition potential to built-up based on (a) AHP and (b) FAHP

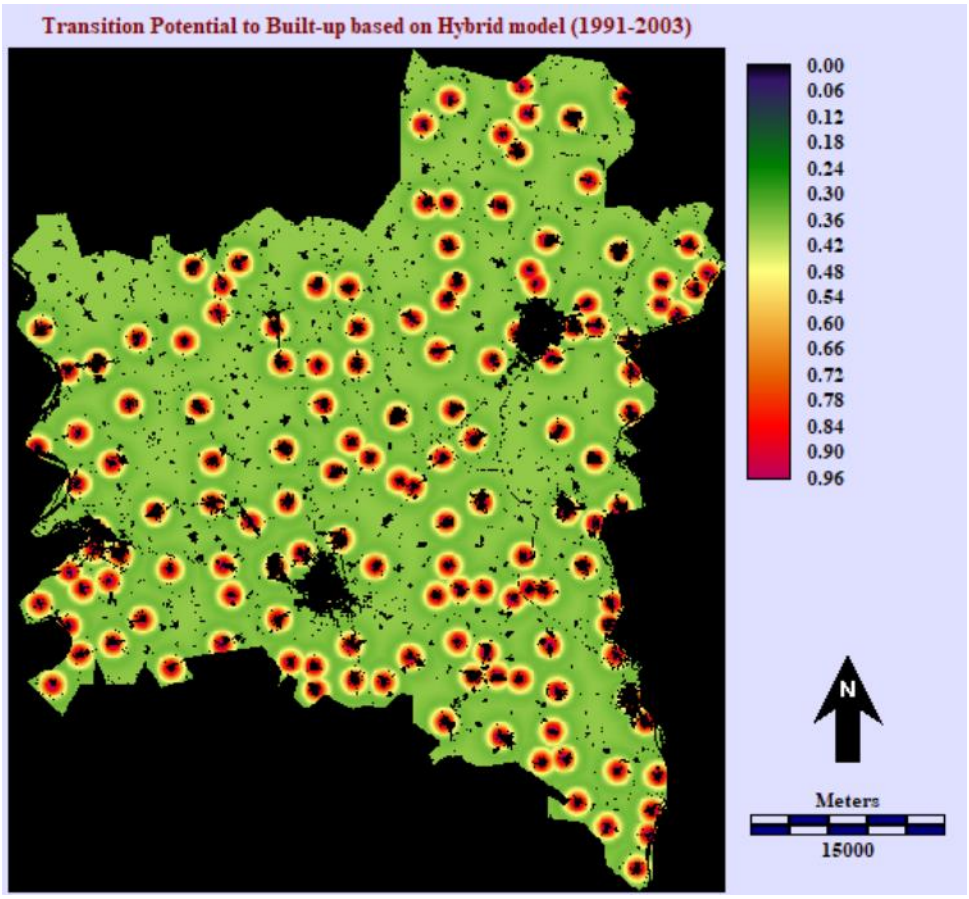


***Figure S2.*** *Transition potential to built-up based on FAHP-CA-Markov chain hybrid model for the calibration period of 1991-2003*

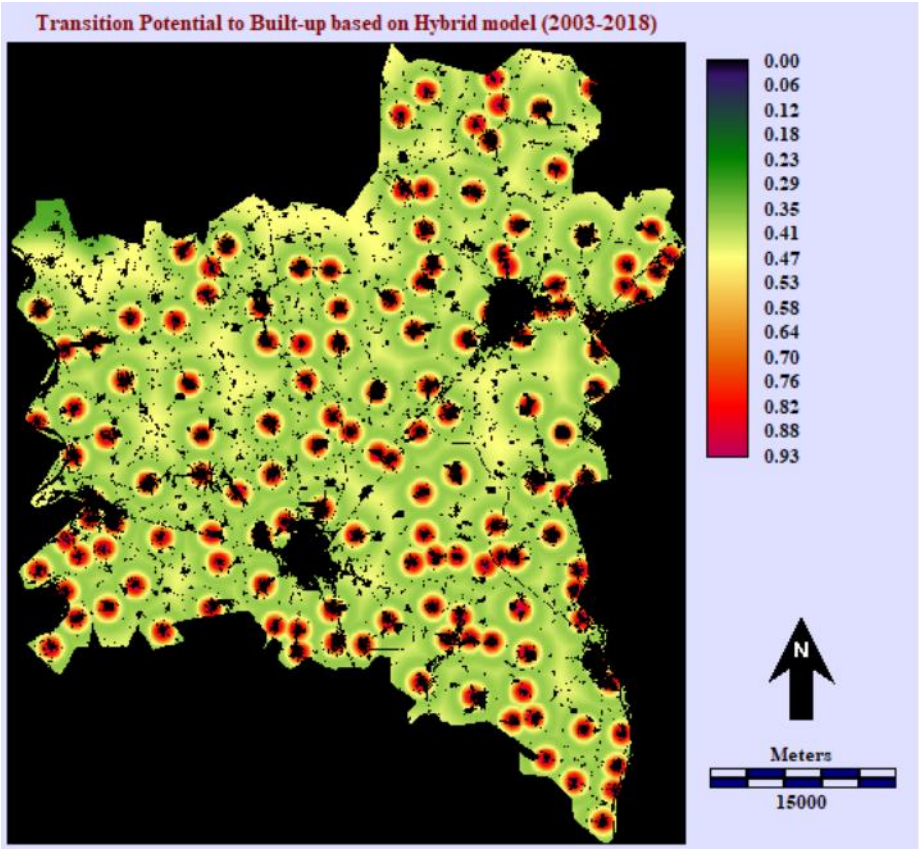


***Figure S3***. *Transition potential to built-up based on FAHP-CA-Markov chain hybrid model for the simulation period of 2003-2018*

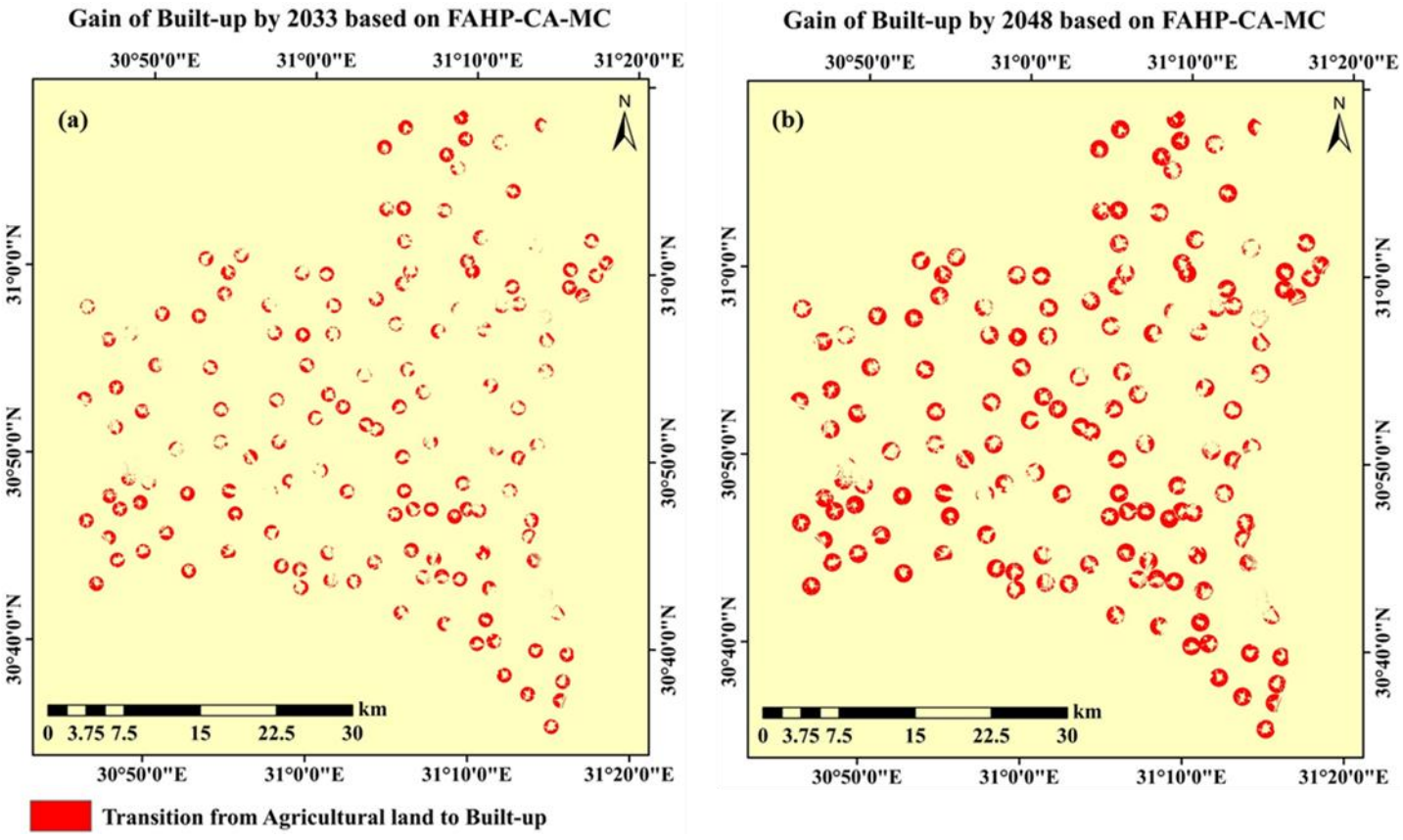


***Figure S4.*** *The gain of built-up obtained based on FAHP-CA-Markov chain model by (a) 2033; (b) 2048*

Table S13. Land Surface Temperature (LST) statistics based on Landsat multitemporal images

| Captured Image | Max Temp (℃) | Min Temp (℃) | Mean Temp (℃) | St. Deviation | $\mu + 0.5*\delta$ |
|---|---|---|---|---|---|
| 1991 | 38.89 | 23.13 | 29.47 | 1.89 | 30.42 |
| 2003 | 46.12 | 26.95 | 33.00 | 2.59 | 34.30 |
| 2018 | 51.81 | 27.94 | 37.92 | 3.15 | 39.50 |

Table S14. The mean and standard deviation of the LST for each district over the three dates, and the computed thresholds.

| District/ mean LST | μ1991 | σ 1991 | $\mu + 0.5*\delta$ | μ2003 | σ 2003 | $\mu + 0.5*\delta$ | μ2018 | σ 2018 | $\mu + 0.5*\delta$ |
|---|---|---|---|---|---|---|---|---|---|
| Basun | 30.05 | 1.95 | 31.03 | 32.69 | 1.98 | 33.68 | 38.32 | 3.23 | 39.94 |
| Kafr elzayat | 29.65 | 1.95 | 30.63 | 34.66 | 2.60 | 35.96 | 39.53 | 3.14 | 41.10 |
| Mahalla Kubra | 28.95 | 1.83 | 29.87 | 31.62 | 2.32 | 32.78 | 36.95 | 3.08 | 38.49 |
| Qotur | 29.68 | 1.87 | 30.62 | 32.14 | 2.10 | 33.19 | 38.19 | 2.86 | 39.62 |
| Samanod | 28.70 | 1.71 | 29.56 | 32.25 | 2.20 | 33.35 | 37.02 | 3.13 | 38.59 |
| Santa | 29.49 | 1.68 | 30.33 | 33.64 | 2.30 | 34.79 | 37.84 | 3.06 | 39.37 |
| Tanta | 30.14 | 1.89 | 31.09 | 33.93 | 2.65 | 35.26 | 38.17 | 3.06 | 39.70 |
| Zefta | 29.45 | 1.73 | 30.32 | 34.18 | 2.44 | 35.40 | 38.56 | 2.98 | 40.05 |

The following eight figures (figure S5 to S12) represent the UHI spatial distribution through the eight districts. The pixels of white color represent the non-UHI where these pixels have LSTs less than the threshold.

Those figures S5, S6, S7, S8, S9, S10, S11, and S12 represent the dimensions and the corresponding LSTs for the districts of Mahalla Kubra, Tanta, Zefta, Kafr Elzayat, Qotur, Samanod, Basun, and Santa respectively. In the figures, a, b and c represent UHI intensities in 1991, 2003, and 2018 respectively, while d, e, and f are the zoom on the most densely populated area for more clarification of the spatial distribution of LST ranges.

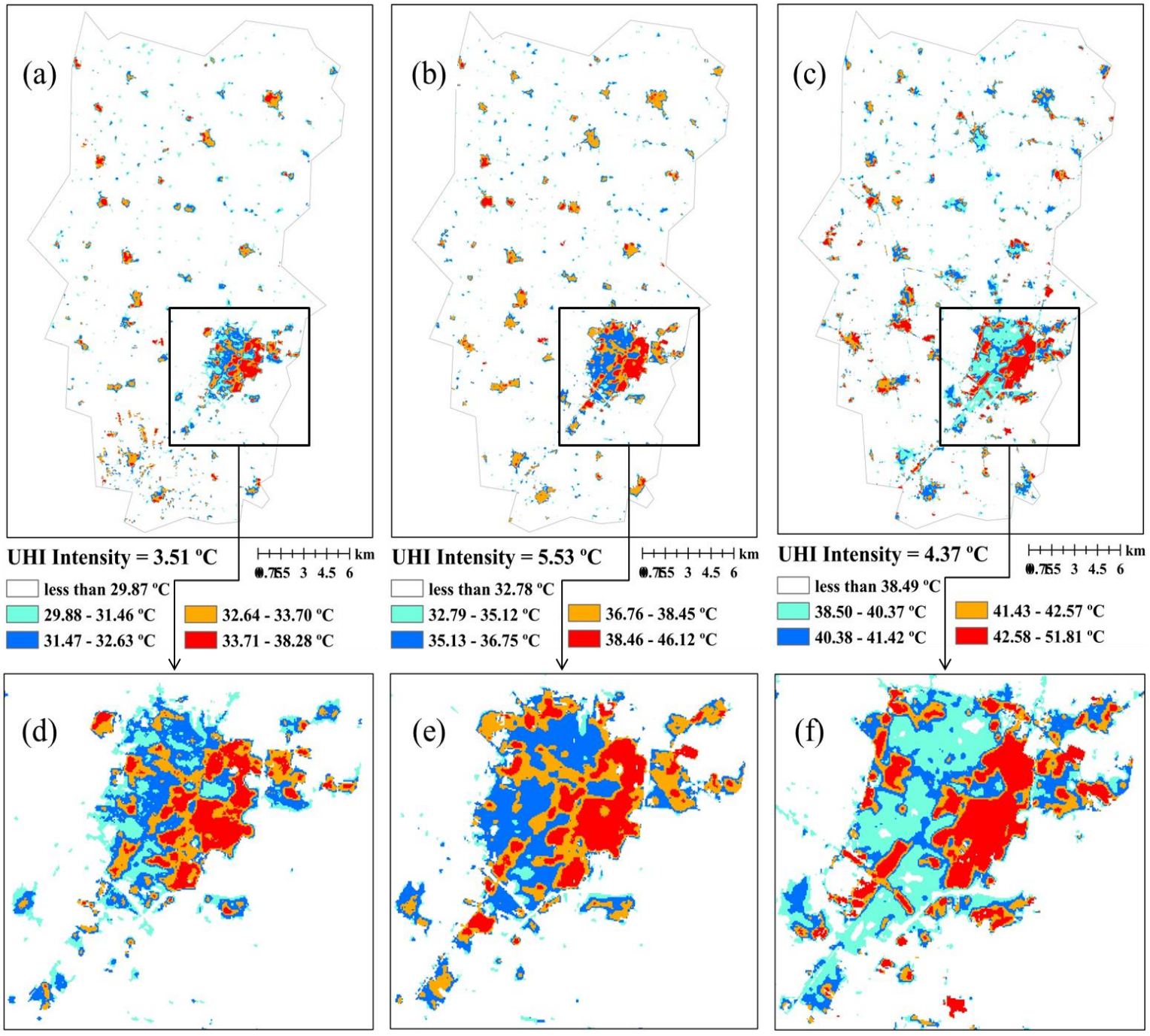


Figure S5. (a), (b) and (c) UHI intensities for Mahalla Kubra in 1991, 2003, and 2018 respectively, while (d), (e), and (f) are the zoom on the most densely populated area.

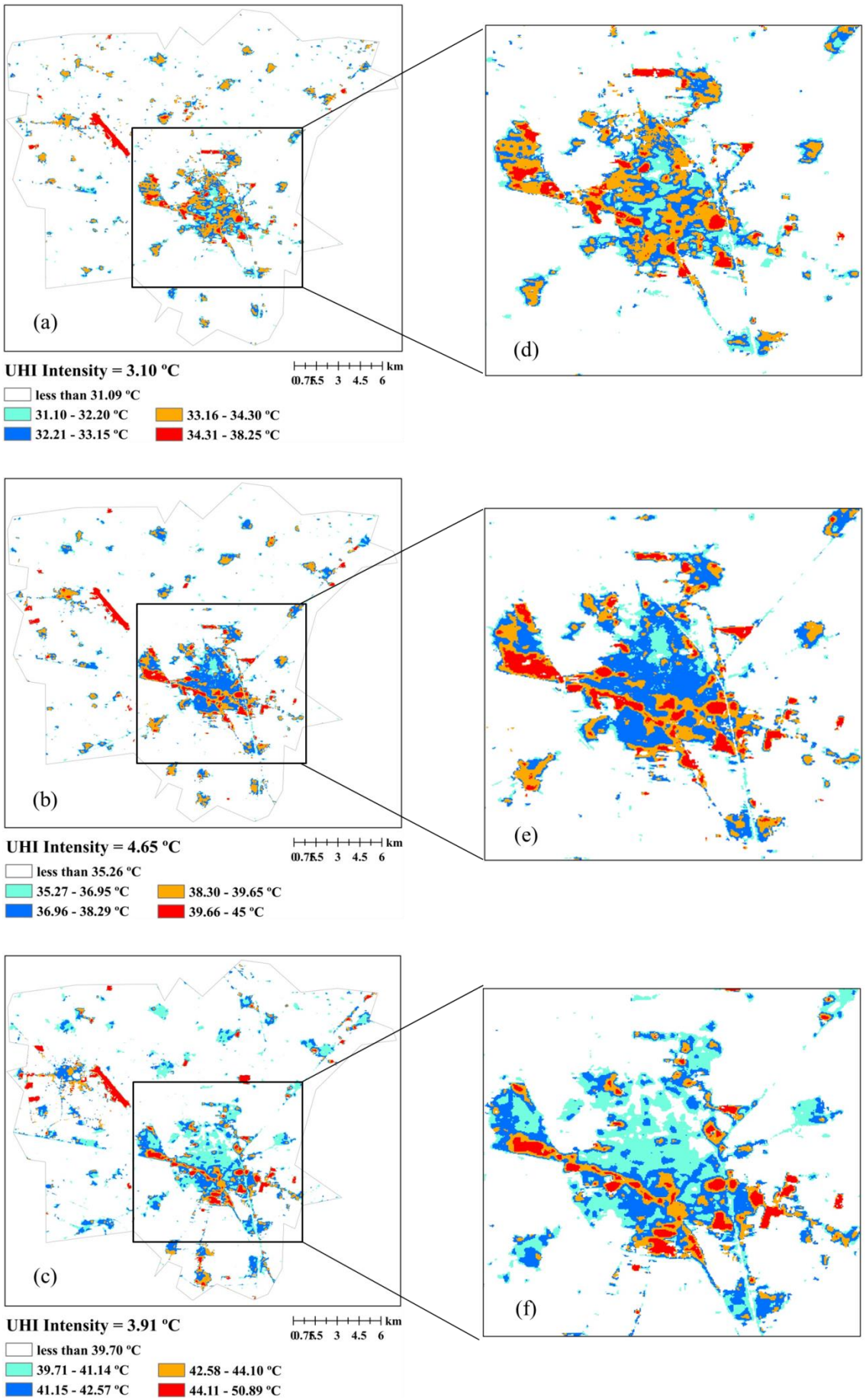


Figure S6. (a), (b) and (c) UHI intensities for Tanta in 1991, 2003, and 2018 respectively, while (d), (e), and (f) are the zoom on the most densely populated area

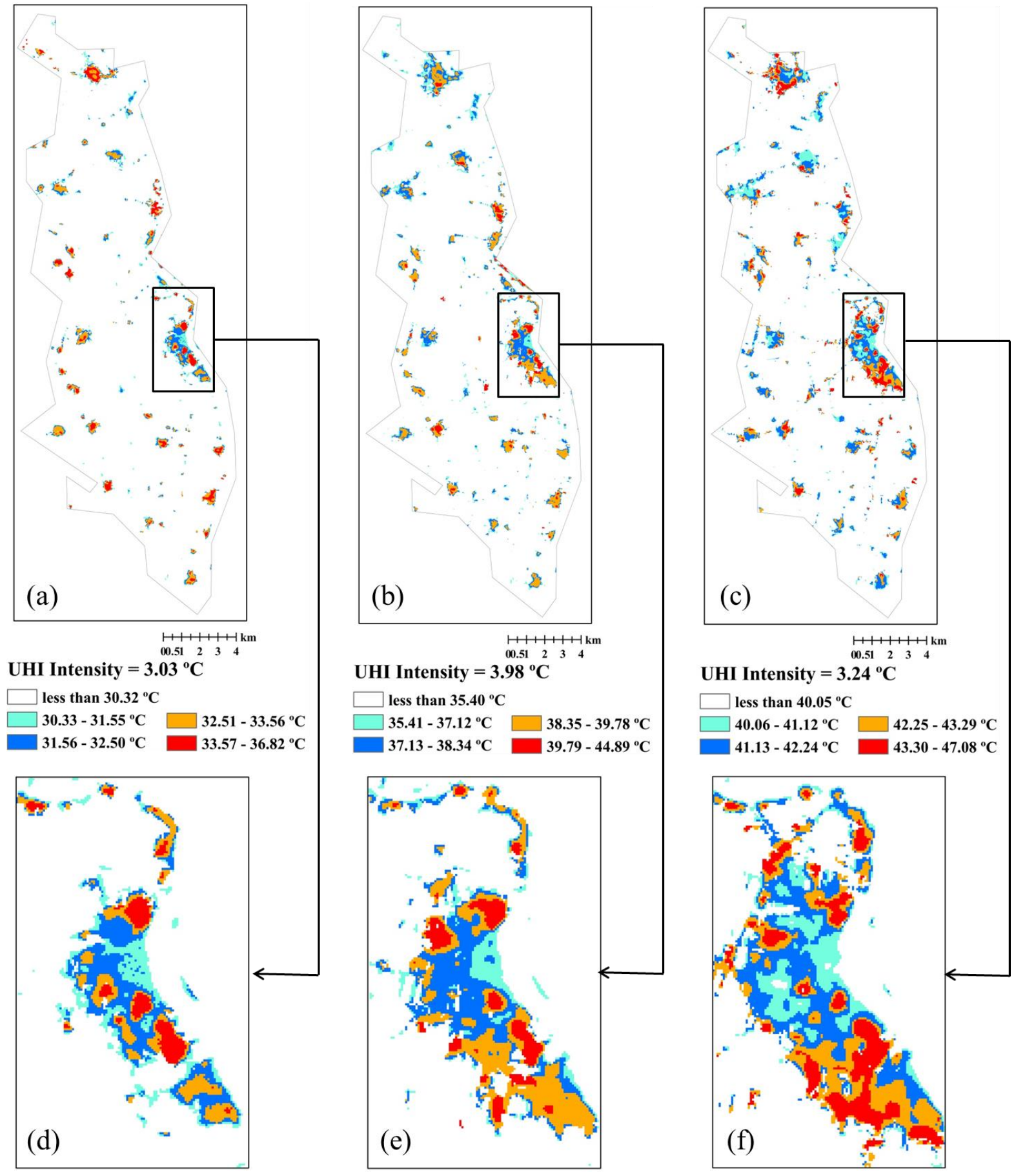


Figure S7. (a), (b) and (c) UHI intensities for Zefta in 1991, 2003, and 2018 respectively, while (d), (e), and (f) are the zoom on the most densely populated area

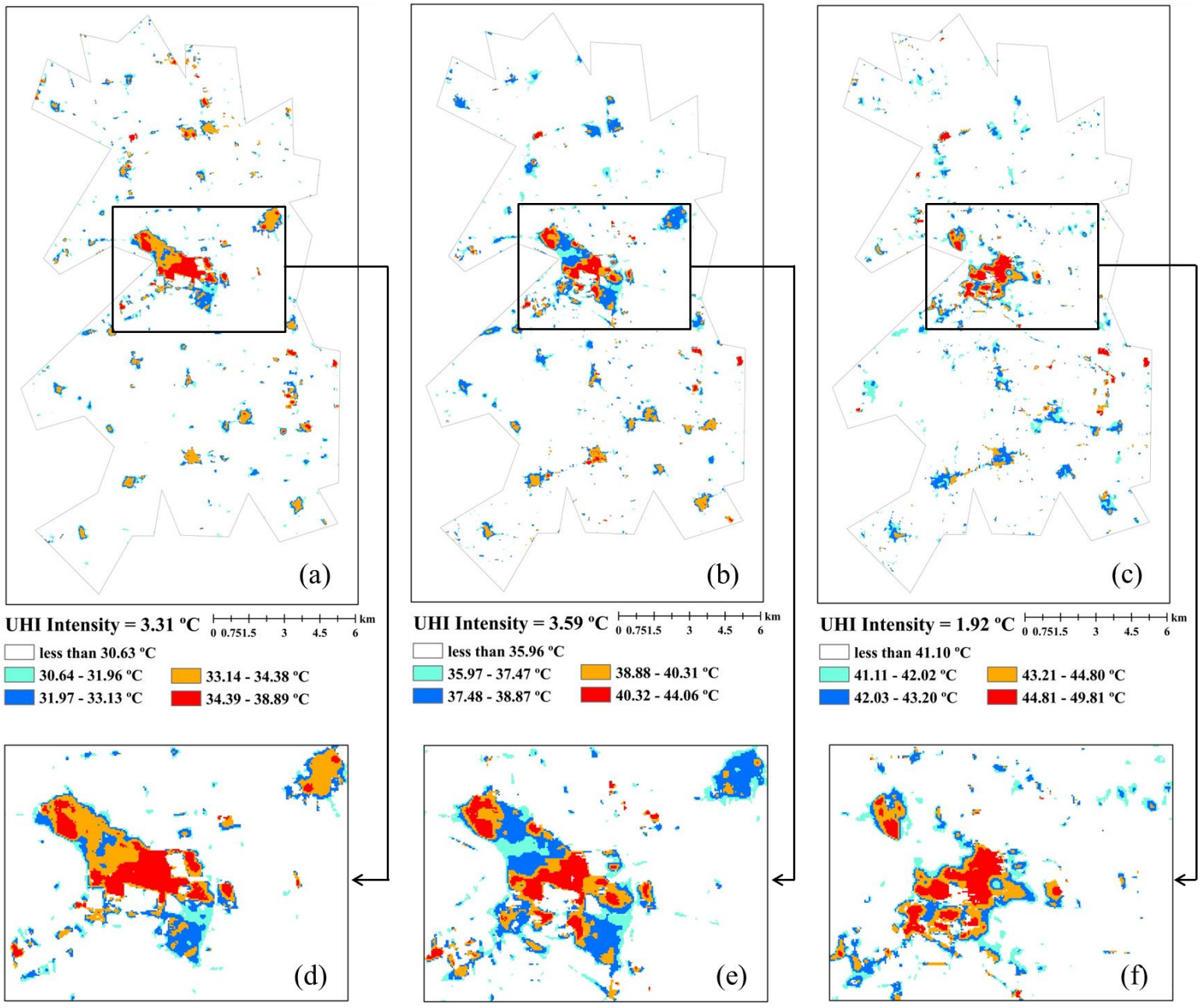


Figure S8. (a), (b) and (c) UHI intensities for Kafr Elzayat in 1991, 2003, and 2018 respectively, while (d), (e), and (f) are the zoom on the most densely populated area.

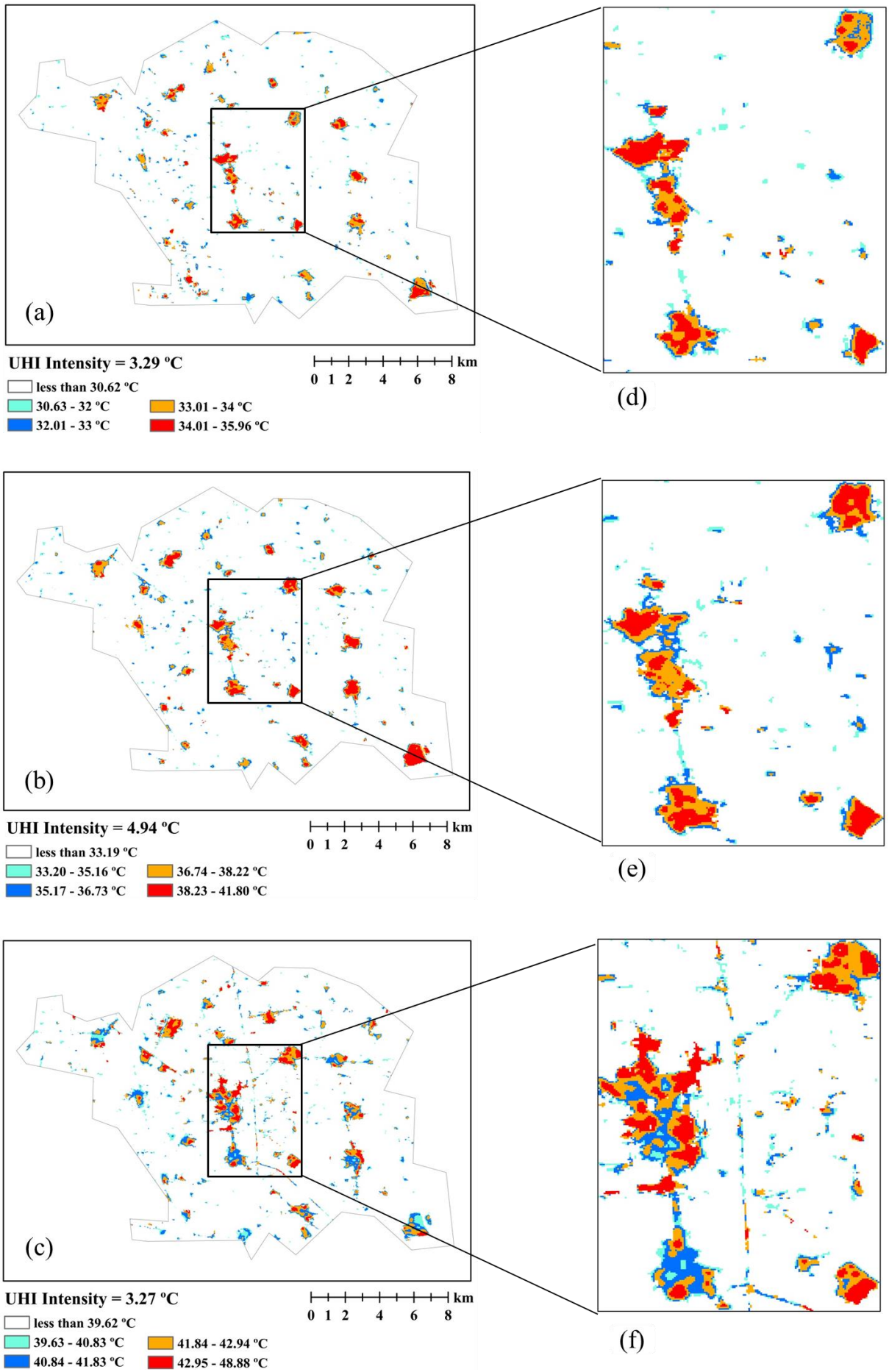


Figure S9. (a), (b) and (c) UHI intensities for Qotur in 1991, 2003, and 2018 respectively, while (d), (e), and (f) are the zoom on the most densely populated area.

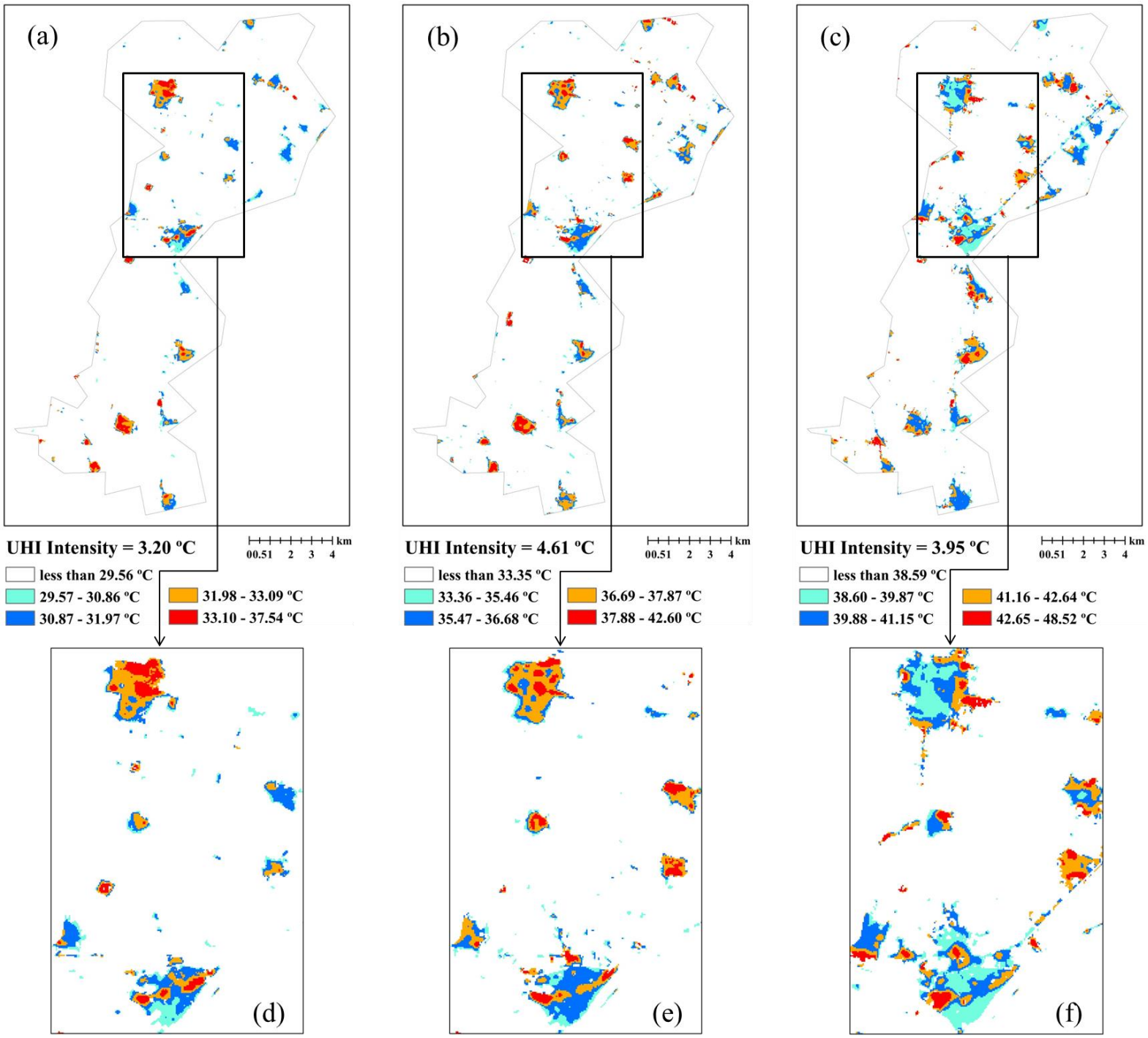


Figure S10. (a), (b) and (c) UHI intensities for Samanod in 1991, 2003, and 2018 respectively, while (d), (e), and (f) are the zoom on the most densely populated area.

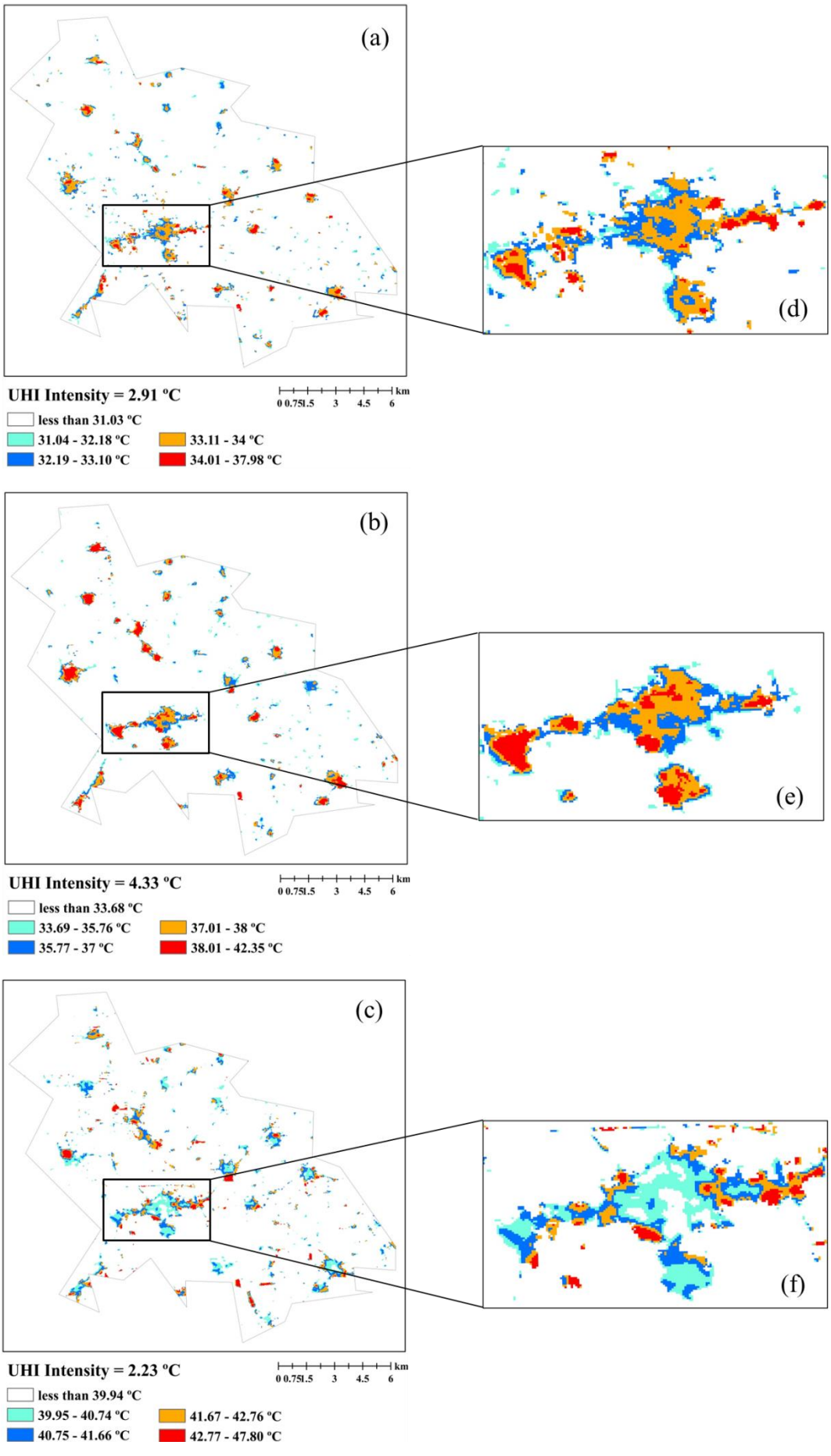


Figure S11. (a), (b) and (c) UHI intensities for Basun in 1991, 2003, and 2018 respectively, while (d), (e), and (f) are the zoom on the most densely populated area.

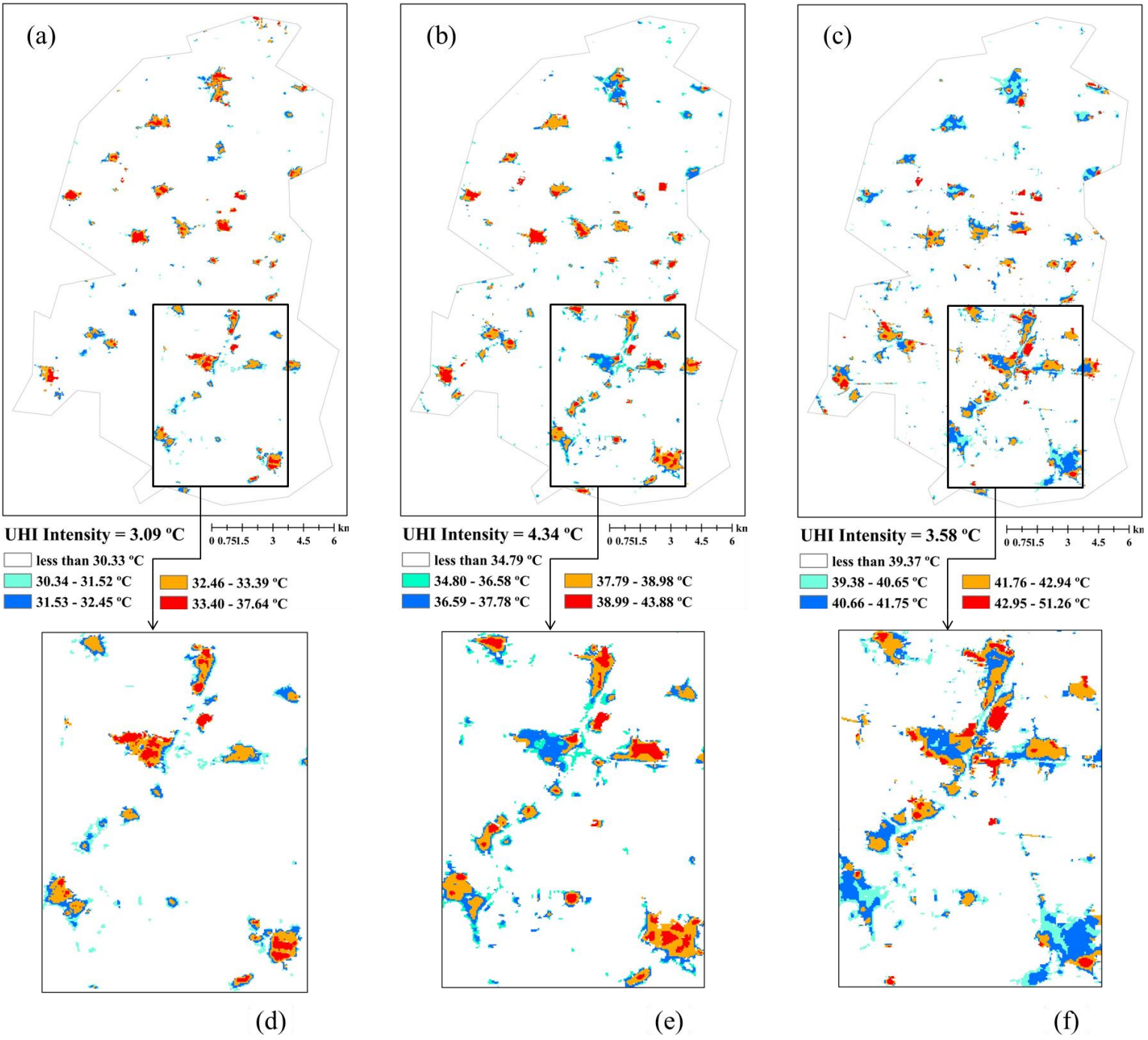


Figure S12. (a), (b) and (c) UHI intensities for Santa in 1991, 2003, and 2018 respectively, while (d), (e), and (f) are the zoom on the most densely populated area.

**Steps of applying FAHP**

1. After creating the fuzzified pairwise comparison matrix of nine criteria selected for the study area, calculating the fuzzy synthetic extent with respect to ith alternative using the following equation (S1)

$$s_i = \sum_{j=1}^{n} a_{ij} \left[\sum_{i=1}^{n} \sum_{j=1}^{n} a_{ij}\right]^{-1} \quad \text{(S1)}$$

where aij is the element of the FPCM of n: no. of criteria.

Table S15. The fuzzy synthetic extent

| Si | *i, m, u* |
|---|---|
| S1 | 0.0110, 0.0143, 0.0199 |
| S2 | 0.1188, 0.182, 0.2788 |
| S3 | 0.108, 0.169, 0.2624 |
| S4 | 0.0639, 0.0914, 0.1353 |
| S5 | 0.0963, 0.1506, 0.2378 |
| S6 | 0.108, 0.1625, 0.246 |
| S7 | 0.0486, 0.0672, 0.0984 |
| S8 | 0.0432, 0.0715, 0.1162 |
| S9 | 0.0594, 0.0867, 0.1312 |

2. Calculating the degree of possibility for a convex fuzzy number to be greater than k convex fuzzy numbers based on equation (S2); figure S10 is a representation of comparable fuzzy numbers:

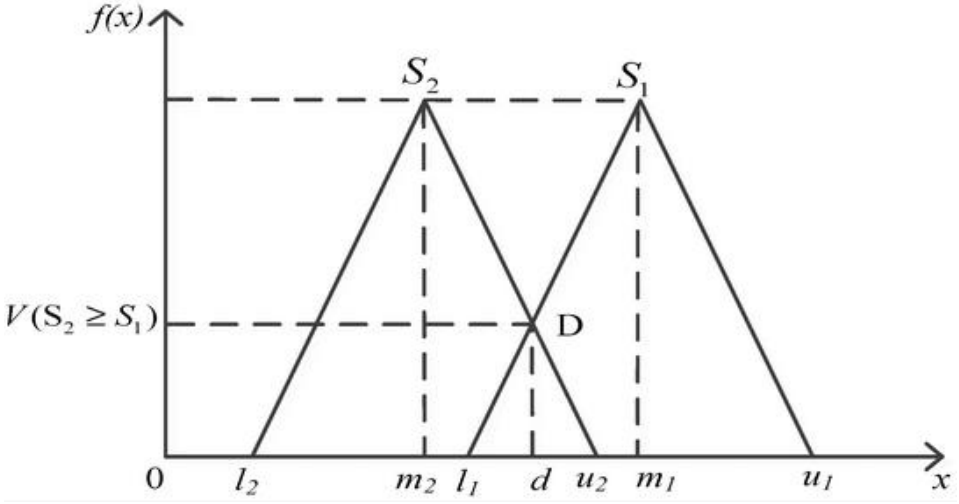


Figure S13. The comparison of two fuzzy numbers

$$V(s_1 \geq s_2) = \sup_{y \geq x}\left[\min\left(\mu_{s_{1(x)}}, \mu_{s_{2(x)}}\right)\right] = hgt(s_1 \cap s_2)$$

$$= \begin{cases} 1 & if\ m_1 \geq m_2, \\ 0 & if\ l_2 \geq u_1, \\ \frac{l_2 - u_2}{(m_1 - u_1) - (m_2 - l_2)}, & 0therwise \end{cases} \qquad \text{(S2)}$$

$$V(S \geq S_1, S_2, S_3 \cdots, S_k) = \min V(S \geq S_i), \qquad i = 1,2,\ldots,k$$

Table S16. The degree of possibility for each fuzzy number to be greater than other fuzzy numbers

| V(S1>Si) | V(S2>Si) | V(S3>Si) | V(S4>Si) | V(S5>Si) | V(S6>Si) | V(S7>Si) | V(S8>Si) | V(S9>Si) |
|---|---|---|---|---|---|---|---|---|
| V(S1>S2)= | V(S2>S1)= | V(S3>S1)= | V(S4>S1)= | V(S5>S1)= | V(S6>S1)= | V(S7>S1)= | V(S8>S1)= | V(S9>S1)= |
| 0 | 1 | 1 | 1 | 1 | 1 | 1 | 1 | 1 |
| V(S1>S3)= | V(S2>S3)= | V(S3>S2)= | V(S4>S2)= | V(S5>S2)= | V(S6>S2)= | V(S7>S2)= | V(S8>S2)= | V(S9>S2)= |
| 0 | 1 | 0.9170 | 0.1541 | 0.7912 | 0.8671 | 0 | 0 | 0.1151 |
| V(S1>S4)= | V(S2>S4)= | V(S3>S4)= | V(S4>S3)= | V(S5>S3)= | V(S6>S3)= | V(S7>S3)= | V(S8>S3)= | V(S9>S3)= |
| 0 | 1 | 1 | 0.2602 | 0.8758 | 0.9550 | 0 | 0.0776 | 0.2199 |
| V(S1>S5)= | V(S2>S5)= | V(S3>S5)= | V(S4>S5)= | V(S5>S4)= | V(S6>S4)= | V(S7>S4)= | V(S8>S4)= | V(S9>S4)= |
| 0 | 1 | 1 | 0.3971 | 1 | 1 | 0.5877 | 0.7244 | 0.9347 |
| V(S1>S6)= | V(S2>S6)= | V(S3>S6)= | V(S4>S6)= | V(S5>S6)= | V(S6>S5)= | V(S7>S5)= | V(S8>S5)= | V(S9>S5)= |
| 0 | 1 | 1 | 0.2774 | 0.9160 | 1 | 0.0246 | 0.2010 | 0.3532 |
| V(S1>S7)= | V(S2>S7)= | V(S3>S7)= | V(S4>S7)= | V(S5>S7)= | V(S6>S7)= | V(S7>S6)= | V(S8>S6)= | V(S9>S6)= |
| 0 | 1 | 1 | 1 | 1 | 1 | 0 | 0.0827 | 0.2343 |
| V(S1>S8)= | V(S2>S8)= | V(S3>S8)= | V(S4>S8)= | V(S5>S8)= | V(S6>S8)= | V(S7>S8)= | V(S8>S7)= | V(S9>S7)= |
| 0 | 1 | 1 | 1 | 1 | 1 | 0.9277 | 1 | 1 |
| V(S1>S9)= | V(S2>S9)= | V(S3>S9)= | V(S4>S9)= | V(S5>S9)= | V(S6>S9)= | V(S7>S9)= | V(S8>S9)= | V(S9>S8)= |
| 0 | 1 | 1 | 1 | 1 | 1 | 0.6667 | 0.7889 | 1 |

3. Calculation of the weight vector using equation (S3) and normalize the nonfuzzy weight vector.

$$d`(A_i) = \min V(S_i \geq S_k),$$

$$W` = (d`(A_1), d`(A_2), \cdots, d`(A_n))^T \qquad \text{(S3)}$$

The minimum values are distinct in italic font in the second row of table 6. The summation of the resulted weights = 3.448, so the weights were normalized to be as follows:

Table S17. The resultant weights based on FAHP

| Criteria | LULC | Dist. to persistent built-up | Dist. to urban centers | Dist. to railway stations | Dist. to nearest road | Neighborhood effect | Population density | Local development | Employment |
|---|---|---|---|---|---|---|---|---|---|
| Weights | 0 | 0.260 | 0.238 | 0.040 | 0.206 | 0.226 | 0 | 0 | 0.030 |

4. Computing (the principal eigenvalue).

The principal eigenvalue can be computed systematically through an equation if the size of the matrix at most is 3*3. In our case, the matrix dimensions are higher, so λmax has been obtained using Matlab.

5. Estimating the consistency index (CI) to measure the inconsistencies of pairwise comparisons using equation (S4)

$$C.I. = \frac{\lambda_{max} - n}{n-1} \quad \text{(S4)}$$

where n is the number of criteria and λmax is the highest eigenvalue.

6. Determining the appropriate value of the random consistency ratio (RI) and calculating the consistency ration (CR).


Figure S14. The shape of the canals inside the study area